

Now, if one is attempting to ballistically match two shells (I and II) to be fired from the same gun,

$$\{I_x/[C_{N\alpha}(X_{cg} - X_{cp})]\}_I = \{I_x/[C_{N\alpha}(X_{cp} - X_{cg})]\}_{II} \quad (10)$$

is required if they are to traverse the same trajectory. If the two shells have essentially the same external shape,

$$[I_x/(X_{cg} - X_{cp})]_I = [I_x/(X_{cp} - X_{cg})]_{II} \quad (11)$$

for identical trajectories. The reader is reminded that while Eq. (10) or (11) is an overriding factor in ballistic matching, neither I_x nor X_{cg} can be changed unless the following conditions remain satisfied:

$$s = [(pI_x/2I)^2/(M\alpha/I)] > 1, \quad \lambda_{1,2} < 0, \quad (12)$$

and

$$(C_D S/W)_I = (C_D S/W)_{II}$$

It is also desirable that $\lambda_{1,2}$ and $\omega_{1,2}$ be roughly matched so that the transient dynamic performance is not changed excessively. The fact that the drag-to-weight ratios must be matched [Eq. (12)] is assumed to be obvious.

Cross Range Drift

It is possible to integrate Eq. (9) when $\bar{\beta}_R$ is constant and obtain an expression for the cross range drift,

$$\mathfrak{D} \cong \iint - (gN_\alpha \bar{\beta}_R/W) dt dt = - (gN_\alpha \bar{\beta}_R/W) (t^2/2) \quad (13)$$

where $N_\alpha = (C_{N\alpha} q' S)$.

It can be shown that for a vacuum trajectory,

$$\dot{\gamma} \cong -g \cos \gamma_0 / V_0 \quad (14)$$

$$t = 2V_0 \sin \gamma_0 / g \quad (15)$$

and

$$V_0 = [gR/(2 \sin \gamma_0 \cos \gamma_0)]^{1/2} \quad (16)$$

Substitution of Eqs. (14-16) into Eq. (13) yields

$$\mathfrak{D} = pI_x (\sin \gamma_0)^{3/2} (2gR)^{1/2} (\cos \gamma_0)^{1/2} / [W(X_{cg} - X_{cp})] \quad (17)$$

where average values for p and $(X_{cg} - X_{cp})$ should be used. Although it is possible to estimate cross range drift of a shell from this equation, it is more useful in predicting the change in drift resulting from perturbations of the shell characteristics. For instance, if it is desired to examine the sensitivity of \mathfrak{D} to changes in I_x , Eq. (17) becomes

$$\mathfrak{D} = CI_x \quad (18)$$

where C is evaluated by calculating a single nominal trajectory. This approach is shown in Fig. 5 compared with 6-dof simulation, and the agreement is excellent. The same approach can be taken with the other shell parameters.

Conclusions

The yaw of repose theory shows that the ratio of roll moment of inertia to the static margin predominates in controlling the yaw of repose angle magnitude in the usual projectile problem. Aside from the drag-to-weight ratio, which dominates any projectile ballistic match problem, the yaw of repose is the single most important projectile parameter.

References

- 1 McShane, E. J., Kelley, J. L., and Reno, F. V., "Exterior Ballistics," University of Denver Press, 1953, pp. 625-631.
- 2 Vaughn, H. R. and Wilson, G. G., "Yaw of Repose on Spinning Shells," SC-RR-70-155, Jan. 1970, Sandia Labs., Albuquerque, N. Mex.
- 3 Nayfeh, A. H., unpublished work on the Dispersion of Reentry Vehicles Caused by Overspin, Aerotherm Corp., Mountain View, Calif., work done under contract to Sandia Corp., PR 48-7754.
- 4 Nicolaides, J. D., "Free Flight Dynamics," Rept. 1966, Aero-Space Dept., Univ. of Notre Dame, Notre Dame, Ind.

⁵ Murphy, C. H., "Free Flight Motion of Symmetric Missiles," Rept. 1216, July 1963, Ballistic Research Labs., Aberdeen Proving Ground, Md.

⁶ Vaughn, H. R., "A Detailed Development of the Tricyclic Theory," SC-M-67-2933, Feb. 1968, Sandia Labs., Albuquerque, N. Mex.

Mass Transfer Effectiveness at Three-Dimensional Stagnation Points

A. WORTMAN*

Northrop Corporation, Hawthorne, Calif.

AND

A. F. MILLS†

University of California, Los Angeles, Calif.

Nomenclature

- C = $(\rho\mu)/(\rho\mu)_e$
 f_i = stream function such that $\partial f/\partial \eta = u_i/u_{ie}$, $i = 1, 2$
 g = enthalpy ratio $H/H_e = h/h_e$
 K = transverse to principal inviscid velocity ratio = α_2/α_1
 M = molecular weight
 Nu = Nusselt number, $q_s Pr_s x_1 / (H_e - h_s) \mu_s$
 q = surface conductive heat flux
 u_i = velocity component
 u = airspeed
 x_i = coordinate; $i = 1, 2$ along surface, $i = 3$ normal to surface
 α_i = inviscid velocity gradient such that $u_{ie} = \alpha_i x_i$, $i = 1, 2$
 λ = heat-transfer parameter, $C_s g_s' / (1 - g_s) Pr_s$
 λ^* = heat-transfer parameter for zero mass transfer
 Λ = normalized heat-transfer parameter, λ/λ^*
 η = transformed coordinate, $(\rho_e \alpha_1 / \mu_e)^{1/2} \int_0^{x_3} (\rho/\rho_e) d\tilde{x}_3$
 ϕ = injection parameter, $-f_s/\lambda^*$
 ω = exponent in viscosity-enthalpy relation

Subscripts

- e = edge of boundary layer
 i = injected species; coordinate direction
 s = surface condition

PRESENTED in this Note are the results of a parametric study of the effectiveness of mass transfer in reducing heat transfer to regular three dimensional stagnation points. The shapes considered here possess two planes of symmetry and range from spheres, through cylinders, to saddle points with equal magnitudes of adverse and favorable pressure gradients. Calculations were performed for model gases ($\rho\alpha h^{-1}$, $\mu\alpha h^\omega$, $Pr = \text{const}$) for wall to total enthalpy ratios ranging up to 0.9, and using real air properties for enthalpy ratios of engineering interest. Our primary objective is to present a simple correlation function appropriate for engineering estimates of mass transfer effects over a wide range of shapes, enthalpy ratios, gas properties, and injection rates. By considering realistic model gases and real air properties in a systematic parametric study, the present contribution stresses heat transfer, in contrast to the study of Libby¹ which employed the simplifying assumption of $\rho\mu = \text{const}$, and focused on enthalpy ratios of 0.0 and 1.0.

The present work follows on that presented in Ref. 2, where heat-transfer correlations were developed for the zero mass transfer situation. The governing equations for three dimensional stagnation point flows are taken directly from

Received November 9, 1970; revision received December 21, 1970.

* Engineering Specialist, Aerodynamics Research Branch. Member AIAA.

† Assistant Professor, School of Engineering and Applied Science. Member AIAA.

Ref. 2, and are

$$(Cf_1'')' + (f_1 + Kf_2)f_1'' + (\rho_e/\rho - f_1'^2) = 0 \quad (1a)$$

$$(Cf_2'')' + (f_1 + Kf_2)f_2'' + K(\rho_e/\rho - f_2'^2) = 0 \quad (1b)$$

$$(Cg'/Pr)' + (f_1 + Kf_2)g' = 0 \quad (1c)$$

subject to the boundary conditions

$$\eta = 0: f_i' = 0, f_i = f_s, g = g_s; i = 1, 2 \quad (2a)$$

$$\eta \rightarrow \infty: f_i' \rightarrow 1.0, g \rightarrow 1.0; i = 1, 2 \quad (2b)$$

The stream functions f_1, f_2 , appear only in a linear combination so that mass transfer at the surface may be assigned to either one, or both. Model gas properties were taken as

$$\rho\alpha h^{-1}; \mu\alpha h^{\omega}, \omega = 0.5, 0.7, 1.0; Pr = 0.7 \quad (3)$$

The equilibrium air density and density-viscosity product were computed from the correlation of Cohen,³ and the total Prandtl number from the polynomial curve-fits of Clutter and Smith.⁴ All the calculations were performed using the method and computer programs developed in Ref. 5. With 151 integration steps across the boundary layer, 4 decimal place accuracy was achieved in about 1 sec of IBM 360/91 computer time per case.

Results and Correlations

It is realized that most practical interest lies in shapes ranging from spheres to cylinders; thus data for saddle shapes ($K < 0$) are included here mainly for completeness. A practical example of a saddle shape is the shape formed by the intersection of a fin and its supporting surface. In order to conveniently exhibit the heat transfer data, we define a heat-transfer function, λ , which in Ref. 2 was found to be only weakly dependent upon gas properties. With the definition

$$\lambda = C_g g_s' / (1 - g_s) Pr_s = (Nu/Re^{1/2}) C_s^{1/2} / Pr_s \quad (4)$$

we have the usual Nusselt-Reynolds number group together with some further accounting for gas property variations. With the definition $\Lambda = \lambda/\lambda^*$ the effect of mass injection on heat transfer may now be considered. Figure 1 shows Λ as a function of K for the model gas at an enthalpy ratio of 0.1, and are typical of the results obtained. It is seen that the effect of gas properties (ω) is pronounced, especially at the high injection rates typical of practical applications such as for reentry vehicles.

The utility of heat-transfer data for engineering calculations is enhanced considerably by the development of adequate correlation functions. It is quite common (e.g., Anfimov⁶) to correlate mass transfer effectiveness as a linear function of injection rate, with corrections for variable property effects expanding the scale of the abscissa. While the simplicity of a linear correlation is quite attractive, it is clear from a cross-plot of Fig. 1 that the linear relation must be limited to relatively low injection rates. In many engineering applications of mass transfer cooling it is desired to reduce convective heat transfer by an order of magnitude, so that correlations extending to high rates of injection should be developed. The form of the correlation function sought here is such that a

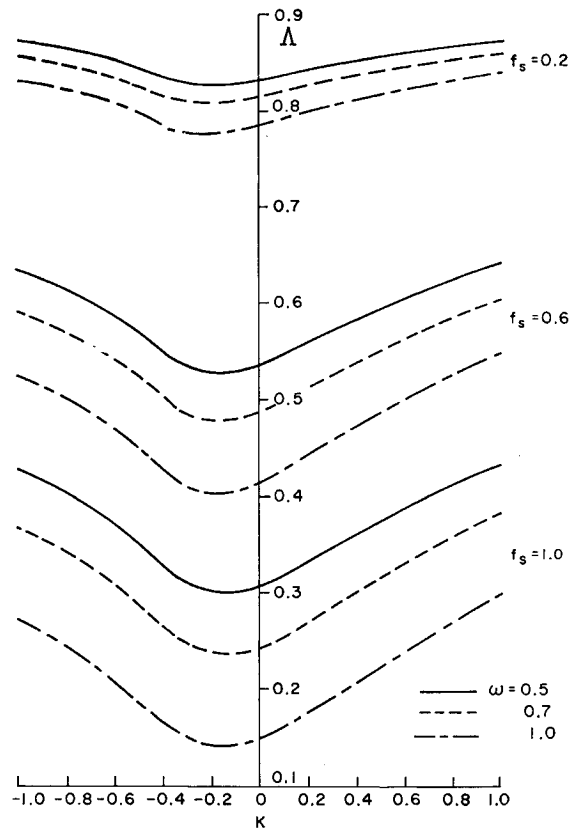


Fig. 1 Effect of mass injection on heat transfer as a function of geometry for various viscosity laws. $Pr = 0.7$.

finite value exists at the origin and the first derivative decays with increase of injection rate until no further change is noticeable for very high injection rates. Exponential functions satisfy these requirements, and indeed are suggested by the results of Couette flow analysis; exponential correlations have been used by a number of authors.⁷ However, for purposes of curve-fitting it is convenient to normalize the injection rate with the heat transfer coefficient, and it is found that use of an Euler transformation on the abscissa allows a linear correlation in the transformed plane. Such a plot is shown in Fig. 2, where the equation of the proposed correlation is

$$1 - \Lambda = 0.63 |f_s/\lambda| / (1 + \frac{2}{3} |f_s/\lambda|) \quad (5)$$

which is within 3% for all the data in the ranges

$$0.05 \leq g_s \leq 0.9; \quad 0.5 \leq \omega \leq 1.0 \quad (6)$$

$$0.0 \leq K \leq 1.0; \quad 0.0 \leq -f_s \leq 2$$

and for real air up to orbital velocities. The data shown in Fig. 2 are representative of the data employed in the development of the correlation function. Close clustering of the points about the curve precluded plotting of all the points considered. Note that the correlation curve quite obviously falls below the data points for ratios of the abscissa greater than about 1.4, which corresponds to $-f_s \leq 2.5$. In order to show the deviation of the $K < 0$ shape data from the results for $K \geq 0$, some representative data points are shown in the figure for $K = -0.6$ and -1.0 .

The correlation function Eq. (5) may be rearranged by solving the quadratic to yield

$$\Lambda = 0.5 \{ 1 - \frac{2}{3} \phi + [(1 - \frac{2}{3} \phi)^2 + \frac{1}{75} \phi]^2 \} \quad (7)$$

where $\phi = -f_s/\lambda^*$ is now viewed as the injection parameter in order to obtain an explicit relation for the mass transfer effectiveness. It remains to prescribe a correlation for the zero mass transfer heat transfer coefficient λ^* . It was shown in Ref. 2 that heat-transfer data for real air and model gases

Table 1 Heat-transfer parameter λ^*

$C = 1.0; Pr = 0.7; \rho\alpha h^{-1}$

K	$g_s = h/H_e$					
	0.01	0.1	0.2	0.4	0.6	0.8
1.0	0.8667	0.8751	0.8854	0.9035	0.9203	0.9360
0.6	0.7760	0.7843	0.7933	0.8100	0.8255	0.8485
0.2	0.6768	0.6853	0.6944	0.7111	0.7265	0.7405
0.0	0.6243	0.6339	0.6440	0.6623	0.6790	0.6945
-0.5	0.5362	0.5547	0.5728	0.6035	0.6295	0.6525
-0.75	0.6058	0.6203	0.6353	0.6623	0.6890	0.7110
-1.0	0.6987	0.7130	0.6601	0.7540	0.7865	0.8075

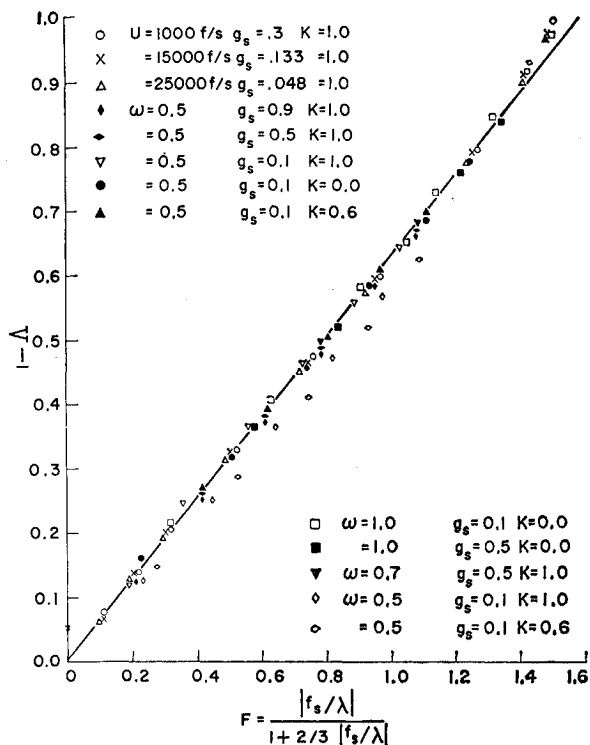


Fig. 2 Correlation of mass transfer effectiveness data for model and real gases.

($1 \leq C_s \leq 5.0$) for all shapes ($-1.0 \leq K \leq 1.0$) could be simply correlated to within 4% by

$$\lambda^*/\lambda^*_{(C=1.0, Pr=0.7)} = 0.12(C_s - 1)^{1/2} \quad (8)$$

The required λ^* data for $C = 1.0$, $Pr = 0.7$, is given in Table 1. The correlation function, Eq. (7), together with Eq. (8) and Table 1 allow the surface heat transfer to be calculated.

Data for homogeneous boundary layers, or air into air injection, have rather limited direct applicability; relatively few engineering systems, outside the field of air-breathing propulsion, are likely to use air as a coolant. More commonly an ablating material is used and the resulting mixture of gases entering the boundary layer may have properties which differ significantly from those of air. At present there are no data for foreign gas injection at three-dimensional stagnation points, but, by use of existing axisymmetric results, the applicability of the present correlation can be extended in an approximate manner. For example, Anfimov⁶ showed that the effect of foreign gas injection on the conductive heat transfer to the surface can be accounted for if the injection parameter is redefined as $\phi' = (f_s/\lambda^*)(M_{air}/M_i)^{0.24}$. Thus it is tentatively proposed that for foreign gas injection into air, ϕ in Eq. (7) be replaced by ϕ' .

References

- Libby, P. A., "Heat and Mass Transfer at a General Three-Dimensional Stagnation Point," *AIAA Journal*, Vol. 7, No. 3, March 1967, pp. 507-517.
- Wortman, A., "Boundary Layer Flow at Three-Dimensional Stagnation Points in High Speed Air Streams," AIAA Paper 70-809, Los Angeles, Calif., 1970.
- Cohen, N. B., "Boundary-Layer Similar Solutions and Correlation Equations for Laminar Heat Transfer Distribution in Equilibrium Air at Velocities up to 41,100 Feet per Second," TR-118, 1961, NASA.
- Clutter, D. W. and Smith, A. M. O., "Solutions of the General Boundary-Layer Equations for Compressible Laminar Flow Including Transverse Curvature," Rept. LB-31088, 1963, Douglas Corp., Long Beach, Calif.
- Wortman, A., "Mass Transfer in Self-Similar Boundary-Layer Flows," Ph.D. dissertation, 1969, School of Engineering and Applied Science, Univ. of California, Los Angeles, Calif.

⁶ Anfimov, N. A., "Heat and Mass Transfer Near the Stagnation Point with Injection and Suction of Various Gases Through the Body Surface," *Mekhanika Zhidkosti i Gaza*, Vol. 1, Jan. 1966, pp. 22-31.

⁷ Gomez, A. V., Mills, A. F., and Curry, D. M., "Correlations of Heat and Mass Transfer for the Stagnation Region of a Re-entry Vehicle with Multicomponent Mass Addition," *Space Systems and Thermal Technology for the 70's*, Pt. II, ASME, June 1970.

Approximate Solution for Coupled Librations of an Axisymmetric Satellite in Circular Orbit

V. J. MODI* AND S. K. SHRIVASTAVA†
University of British Columbia,
Vancouver, B. C., Canada

Nomenclature†

- x, y, z = principal axes, with z along the axis of symmetry
 A_i = functions of ψ, ψ', ϕ, ϕ'
 B_f = aerodynamic coefficient¹
 C_1 = constant, $\pi/2 \{(1 - K_i)/3(1 + K_i)\}^{1/2}$
 C_H = nondimensionalized Hamiltonian, $2H/I\theta^2$
 H = Hamiltonian
 K_i = inertia parameter, $1 - I_{xx}/I$ where $I = I_{xx} = I_{yy} > I_{zz}$
 θ = angular position of the satellite as measured from pericenter
 θ_1^*, θ_2^* = phase angles
 ϕ = rotation across the orbital plane (roll)
 ψ = rotation in the orbital plane (pitch)
 λ = rotation about z axis (yaw)

Introduction

ATTITUDE dynamics² of gravity-oriented satellites has been studied extensively in recent years.³ The complexity of the problem has, in most cases, led to the use of numerical techniques.^{1,4} However, the digital approach often fails to give an insight into the system behavior in absence of extensive computations which tend to be rather expensive.

Here, a simple approximate analytical method using the constant Hamiltonian of the system is proposed to solve a set of nonlinear, coupled equations corresponding to the general librations of a satellite.

Analysis

For a rigid, nonspinning, axisymmetric satellite negotiating a circular trajectory in the gravity gradient field with the atmospheric effect, the equations of the librational motion, with θ as the independent variable, are¹

$$\psi'' - 2\phi'(\psi' + 1) \tan\phi + 3K_i \sin\psi \cos\psi + B_f(|\cos\psi| + C_1 \sin\psi) \cos\psi/\cos^2\phi = 0 \quad (1a)$$

$$\phi'' + \{(\psi' + 1)^2 + 3K_i \cos^2\psi\} \sin\phi \cos\phi = 0 \quad (1b)$$

$$\lambda' - (1 + \psi') \sin\phi = 0 \quad (1c)$$

Recognizing that the Eqs. (1a) and (1b) do not involve λ explicitly, their solution can be undertaken independent of Eq. (1c). Multiplying them by $2\psi' \cos^2\phi$ and $2\phi'$, respectively, adding and integrating once yield the normalized

Received December 8, 1970; revision received February 16, 1971. The research for this paper was supported (in part) by the Defence Research Board of Canada, Grant 9551-18.

* Professor. Member AIAA.

† Post-doctoral Fellow. Associate Member AIAA.

‡ Primes indicate differentiation with respect to θ ; subscript e represents equilibrium condition.